Arabian Journal of Chemistry (2010) 3, 103–113

King Saud University

Arabian Journal of Chemistry

www.ksu.edu.sa
www.sciencedirect.com

ORIGINAL ARTICLE

Synthesis and spectroscopic characterization of new tetradentate Schiff base and its coordination compounds of NOON donor atoms and their antibacterial and antifungal activity

Sayed M. Abdallah [a], M.A. Zayed [b,*], Gehad G. Mohamed [b]

[a] *Workers University, Aswan, Egypt*
[b] *Chemistry Department, Faculty of Science, Cairo University, 12613 Giza, Egypt*

Received 21 January 2009; accepted 19 July 2009
Available online 10 February 2010

KEYWORDS

Schiff base;
Transition metal complexes;
Spectroscopy;
Molar conductance;
Thermal analysis;
Biological activity

Abstract New Schiff base (H_2L) ligand is prepared via condensation of *o*-phthaldehyde and 2-aminobenzoic acid in 1:2 ratio. Metal complexes are prepared and characterized using elemental analyses, IR, solid reflectance, magnetic moment, molar conductance, ^{1}H NMR, ESR and thermal analysis (TGA). From the elemental analyses data, the complexes were proposed to have the general formulae $[MCl(L)(H_2O)]\cdot 2H_2O$ (where M = Cr(III) and Fe(III)); $[M(L)]\cdot yH_2O$ (where M = Mn(II), Ni(II), Cu(II) and Zn(II), y = 1–2) and $[M(L)(H_2O)_n]\cdot yH_2O$ (where M = Co(II) ($n = y = 2$), Co(II) ($n = y = 1$), Ni(II) ($n = 2$, $y = 1$). The molar conductance data reveal that all the metal chelates were non-electrolytes. IR spectra show that H_2L is coordinated to the metal ions in a bi-negative tetradentate manner with NOON donor sites of the azomethine-N and carboxylate-O. The ^{1}H NMR spectral data indicate that the two carboxylate protons are also displaced during complexation. From the magnetic and solid reflectance spectra, it was found that the geometrical structure of these complexes are octahedral (Cr(III), Fe(III), Co(II) and Ni(II)), square planar (Cu(II)), trigonal bipyramidal (Co(II)) and tetrahedral (Mn(II), Ni(II) and Zn(II)). The thermal behaviour of these chelates showed that the hydrated complexes losses water molecules of hydration in the first step followed immediately by decomposition of the ligand molecule in the subsequent

* Corresponding author.
E-mail address: mazayed429@yahoo.com (M.A. Zayed).

doi:10.1016/j.arabjc.2010.02.006

Production and hosting by Elsevier

steps. The biological activity data show that the metal complexes to be more potent/antibacterial than the parent Shciff base ligand against one or more bacterial species.

1. Introduction

A large number of Schiff bases (Sonmez et al., 2003; Vaghasiya et al., 2004; Elerman and Kabak, 2002) and their complexes have been investigated for their interesting and important properties, such as their ability to reversibly bind oxygen, catalytic activity in the hydrogenation of olefins, photochromic properties and complexing ability towards some toxic metals.

Furthermore, complexes of Schiff bases showed promising biological activity and biological modeling applications (Khalil et al., 2005; Chantarasiri et al., 2004; Soliman, 2001; Soliman and Mohamed, 2004; Tas et al., 2004).

The Schiff base ligands with sulphur and nitrogen donor atoms in their structures act as good chelating agents for the transition and non-transition metal ions (Kaushik and Mishra, 2003; Manav et al., 2000; Mishra et al., 2005; Abd El Wahed et al., 2004). Coordination of such compounds with metal ions, such as copper, nickel and iron, often enhances their activities (Singh et al., 2000), as has been reported for pathogenic fungi (Patel and Parekh, 2005). There is a continuing interest in metal complexes of Schiff bases. Because of the presence of both hard nitrogen or oxygen and soft sulphur donor atoms in the backbones of these ligands, they are readily coordinate with a wide range of transition metal ions yielding stable and intensely coloured metal complexes. Some of which have been shown to exhibit interesting physical and chemical properties (Tian et al., 1997) and potentially useful biological activities (Karabocek et al., 1997).

Many reports are available for the preparation and properties of model copper complexes which mimic copper-containing metalloproteins such as hemocyanine and tyrosinase. Two noticeable properties of copper proteins show an intense absorption band (Kaizer et al., 2007) near 600 nm and relatively high copper(II)/copper(I) reduction potentials (Tian et al., 1997). Attention was particularly focused on their correlation with the active site of metalloenzymes and metalloproteins containing dinuclear metallocenters. This attention is important to elucidate the factors that determine the reversible binding and activation of O_2 in various natural oxygen transport systems and mono- and dioxygenases and to mimic their activity (Kaizer et al., 2007).

Schiff bases (Sixt and Kaim, 2000) were still regarded as one of the most potential group of chelators for facile preparations of metallo-organic hybrid materials. The interest in Schiff base compounds as analytical reagents is increasing since they enable simple and unexpensive determinations of different organic and inorganic substances (Estrela et al., 2003). The high affinity for the chelation of the Schiff bases towards the transition metal ions is utilized in preparing their solid complexes.

As an extension of our work on the structural characterization of Schiff base ligands and their metal complexes (Mohamed, 2006; Soliman and Mohamed, 2004; Mohamed and Sharaby, 2007), the main target of the present article is to study the coordination behaviour of a new and novel H_2L Schiff base that incorporate several binding sites towards Cr(III), Mn(II), Fe(III), Co(II) and Ni(II) (Cl and ClO_4), Cu(II) and Zn(II) ions. Also to evaluate the relative thermal stability of the synthesized complexes and to examine their antimicrobial activity against different species of bacteria and fungi.

2. Experimental

2.1. Materials and reagents

All chemicals used were of the analytical reagent grade (AR). They included *o*-phthaldehyde (Sigma); 2-aminobenzoic acid (Sigma); copper(II) chloride dihydrate (Prolabo); cobalt(II) and nickel(II) chlorides hexahydrates (BDH); cobalt(II) and nickel(II) perchlorates hexahydrates (Sigma); zinc(II) chloride dihydrate (Ubichem), chromium(III) chloride hexahydrate (Sigma); manganese(II) chloride and ferric(III) chloride hexahydrate (Prolabo). Zinc oxide, EDTA (AnalaR), ammonia solution (33% v/v) and ammonium chloride were supplied from El-Nasr Pharm. Chem. Co., Egypt. Organic solvents used included absolute ethyl alcohol, diethylether, and dimethylformamide (DMF). These solvents were spectroscopic pure from BDH. Hydrogen peroxide, hydrochloric and nitric acids (MERCK) were used. De-ionized water collected from all glass equipments was usually used in all preparations.

2.2. Instruments

The molar conductance of solid complexes in DMF (10^{-3} M) was measured using Sybron–Barnstead conductometer (Meter-PM.6, $E = 3406$). Elemental microanalyses of the separated solid chelates for C, H, N and S were performed in the Microanalytical Center, Cairo University. The analyses were repeated twice to check the accuracy of the data. Infrared spectra were recorded on a Perkin–Elmer FT-IR type 1650 spectrophotometer in the region 4000–400 cm^{-1} as KBr discs. The solid ESR spectra of the complexes were recorded with ELEXSYS E500 Bruker spectrometer in 3 mm Pyrex tubes at 298 K. Diphenylpicrydrazide (DPPH) was used as a g-marker for the calibration of the spectra. The ^1H NMR spectra were recorded with a JEOL EX-270 MHz in d_6-DMSO as solvent, where the chemical shifts were determined relative to the solvent peaks. The solid reflectance spectra were measured on a Shimadzu 3101 pc spectrophotometer. The molar magnetic susceptibility was measured on powdered samples using the Faraday method. The diamagnetic corrections were made by Pascal's constant and $Hg[Co(SCN)_4]$ was used as a calibrant. The magnetic data for the background of the sample holder were corrected. The thermogravimetric analysis (TGA and DrTGA) was carried out in dynamic nitrogen atmosphere (20 ml min^{-1}) with a heating rate of 10 °C min^{-1} using Shimadzu TGA-50H thermal analyzers.

2.3. Synthesis of the Schiff base (H_2L)

Hot solution (60 °C) of 2-aminobenzoic acid (2.74 g, 20 mmol) was mixed with hot solution (60 °C) of *o*-phthaldehyde (1.34 g,

10 mmol) in 50 ml ethanol. The resulting mixture was left under reflux for 4 h and the solvent was evaporated till deep yellow oil product is separated. This oil is poured on ice cold dilute HCl whereupon the yellow crystalline product is separated. The formed solid product was separated by filtration, purified by crystallization from ethanol, washed with diethyl ether and dried in a vacuum over anhydrous calcium chloride. The yellow product is produced in 86% yield.

2.4. Synthesis of metal complexes

The metal complexes were prepared by the addition of hot solution (60 °C) of the appropriate metal chloride or perchlorate (1 mmol) in an ethanol–water mixture (1:1, 25 ml) to the hot solution (60 °C) of the Schiff base (0.372 g, 1 mmol) in the same solvent (25 ml). The resulting mixture was stirred under reflux for one hour whereupon the complexes precipitated. They were collected by filtration, washed with a 1:1 ethanol: water mixture and diethylether. The microanalysis data for C, H and N were repeated twice.

2.5. Biological activity

A filter paper sterilized disc saturated with measured quantity of the sample (10 μl, 20 mg/ml) is placed on plate containing solid bacterial medium (nutrient agar broth) or fungal medium (Dox s medium) which has been heavily seeded with spore suspension of the tested organism. The assay plates which incubated at 28 °C for 2 days for yeasts and at 37 °C for 1 day for bacteria. After inoccupation, the diameter of the clear zone of inhibition surrounding the sample is taken as a measure of the inhibitory power of the sample against the particular test organism (Grayer and Harbone, 1994; Irob et al., 1996). The organisms used included Gram-positive (*Staphylococcus aurous*), Gram-negative (*Escherichia coli*) bacteria and Fungi (*Candida albicans* and *Aspergillus flavus*).

3. Results and discussion

3.1. Schiff base characterization

The Schiff base, H_2L, is subjected to elemental analyses. The results of elemental analyses (C, H and N) with molecular formula and the melting points are presented in Table 1. The results obtained are in good agreement with those calculated for the suggested formula. The melting points are sharp indicating the purity of the prepared Schiff base. The scheme of the Schiff base preparation is given by Fig. 1.

The structure of this Schiff base is also confirmed by IR and ^{1}H NMR spectra, which will be discussed in detailed manner together with its metal complexes later. It takes the following structural formula and IUPAC name:

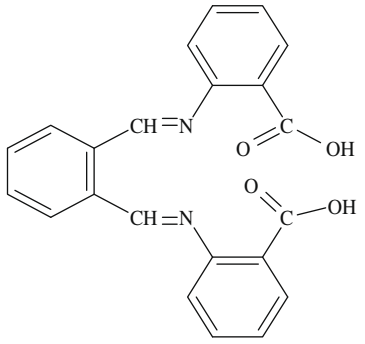

3.2. Composition and structures of Schiff base complexes

The isolated solid complexes of Cr(III), Mn(II), Fe(III), Co(II) and Ni(II) (chlorides and perchlorates), Cu(II) and Zn (II) ions with the Schiff base H_2L ligand were subjected to elemental analyses (C, H, N and metal content), IR, magnetic studies, molar conductance and thermal analysis (TGA), to identify

Table 1 Analytical and physical data of H_2L ligand and its metal complexes.

Compound	m.p. (°C)	Colour (% yield)	% Found (Calcd.)				$\mu_{eff.}$ (B.M.)	$\Omega_m\ \Omega^{-1}\ mol^{-1}\ cm^2$
			C	H	N	M		
H_2L	100	Yellow	70.27	5.07	7.14	—	—	—
($C_{22}H_{16}N_2O_4$)		(86)	(70.47)	(5.30)	(7.53)			
[CrCl(L)(H_2O)]·2H_2O	> 300	Green	51.33	4.11	5.17	9.86		
$C_{22}H_{20}ClCrN_2O_7$		(70)	(51.61)	(3.91)	(5.47)	(10.17)	4.05	10.26
[Mn(L)]·H_2O	> 300	Brown	60.07	3.63	6.64	12.45		
$C_{22}H_{16}MnN_2O_5$		(72)	(59.73)	(3.62)	(6.33)	(12.22)	4.72	10.11
[FeCl(L)(H_2O)]·2H_2O	> 300	Yellowish Brown	50.83	3.76	5.56	11.08		
$C_{22}H_{20}ClFeN_2O_7$		(63)	(51.21)	(3.88)	(5.43)	(10.86)	5.39	9.75
[Co(L)(H_2O)$_2$]·2H_2O	> 300	Reddish brown	52.38	4.31	5.95	12.89		
$C_{22}H_{22}CoN_2O_8$		(59)	(52.69)	(4.39)	(5.59)	(12.69)	5.62	11.25
[Co(L)(H_2O)]·H_2O	> 300	Brown	56.68	4.02	6.35	12.56		
$C_{22}H_{18}CoN_2O_6$		(66)	(56.77)	(3.87)	(6.02)	(12.69)	5.25	12.30
[Ni(L)]·2H_2O	> 300	Green	56.94	3.58	6.43	12.92		
$C_{22}H_{18}NiN_2O_6$		(60)	(56.77)	(3.87)	(6.02)	(12.69)	4.64	6.75
[Ni(L)(H_2O)$_2$]·H_2O	> 300	Yellow	54.39	3.86	5.42	12.56		
$C_{22}H_{20}NiN_2O_7$		(68)	(54.66)	(4.14)	(5.78)	(12.22)	3.67	8.45
[Cu(L)]·1.5H_2O	> 300	Green	57.43	3.47	5.74	13.43		
$C_{22}H_{17}CuN_2O_{5.5}$		(70)	(57.33)	(3.69)	(6.08)	(13.79)	1.93	15.65
[Zn(L)]·H_2O	> 300	Yellow	58.07	3.69	6.37	14.05		
$C_{22}H_{16}N_2O_5Zn$		(58)	(58.28)	(3.53)	(6.18)	(14.35)	diam.	13.64

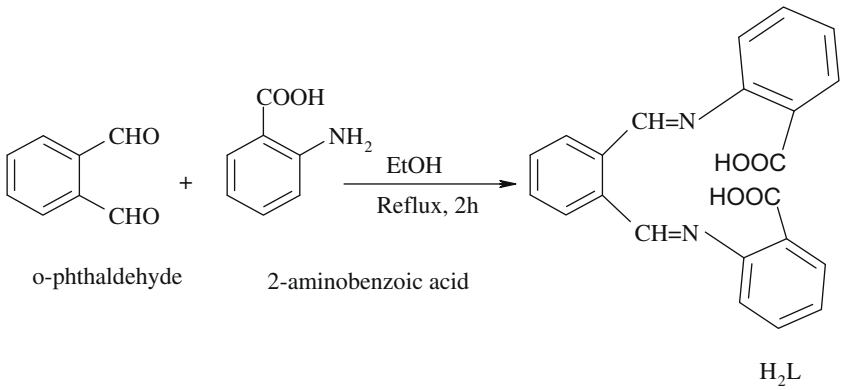

Figure 1 Preparation scheme of H_2L ligand.

their tentative formulae in a trial to elucidate their molecular structures. The results of elemental analyses listed in Table 1 suggest the formulae $[MCl(L)(H_2O)]\cdot 2H_2O$ (where M = Cr(III) and Fe(III)); $[M(L)]\cdot yH_2O$ (where M = Mn(II), Ni(II), Cu(II) and Zn(II), y = 1–2) and $[M(L)(H_2O)_n]\cdot yH_2O$ (where M = Co(II) ($n = y = 2$), Co(II) ($n = y = 1$), Ni(II) ($n = 2$, $y = 1$).

3.3. Molar conductivity measurements

The chelates were dissolved in DMF and the molar conductivities of 10^{-3} M of their solutions at 25 °C were measured. Table 1 shows the molar conductance values of the complexes. The molar conductance values of the complexes fall in the range 6.75–15.65 Ω^{-1} mol^{-1} cm^2 indicating that these chelates are non-electrolytes.

3.4. IR spectral studies

The IR data of the spectra of H_2L Schiff base and its complexes are listed in Table 2. The IR spectra of the complexes are compared with those of the free ligand in order to determine the coordination sites that may involve in chelation. The position and/or the intensities of these peaks are expected to be changed upon chelation. New peaks are also guide peaks as well as water in chelation. These guide peaks are listed in Table 2.

Upon comparison it was found that the azomethine υ(C═N) stretching vibration is found in the free ligand at 1603 cm^{-1}. This band is shifted to lower wavenumbers (1587–1599 cm^{-1}) in the complexes indicating the participation of the azomethine nitrogen in coordination (Mohamed and Sharaby, 2007).

The υ(OH), υ(C═O), υ_{asym}(COO) and υ_{sym}(COO) stretching vibrations are observed at 3300–3400 (broad band), 1682, 1587 and 1393 cm^{-1} for H_2L. The existence of water of hydration and/or water of coordination in the spectra of the complexes render it difficult to get conclusion from the OH group of the H_2L ligand, which will be overlapped by those of the water molecules. The participation of the OH group is further confirmed by clarifying the effect of chelation on the asymmetric and symmetric carboxylic stretching vibrations.

The participation of the carboxylate-O atom in the complexes formation was evidenced from the shift in position of these bands to 3275–3309, 1675–1716, 1502–1556 and 1400–1454 cm^{-1} in the metal complexes (Soliman and Mohamed, 2004). New bands are found in the spectra of the complexes in the regions 484–535 cm^{-1}, which are assigned to υ(M–O) stretching vibrations (Mohamed, 2006; Mohamed and Sharaby, 2007). The bands at 420–488 cm^{-1} have been assigned to υ(M–N) mode Mohamed, 2006; Mohamed and Sharaby, 2007.

Therefore, from the IR spectra, it is concluded that H_2L ligand behaves as a bi-negative tetradentate ligand coordinat-

Table 2 IR spectra (4000–400 cm^{-1}) of the H_2L ligand and its metal complexes.

Compound	ν(C = O)	ν(COO) (asym)	ν(COO) (sym.)	ν(CH = N)	$V(H_2O)$ (coord.)	ν(M–O)	ν(M–N)
H_2L	1682br	1587s	1393sh	1603m	——	——	——
$[CrCl(L)(H_2O)]\cdot 2H_2O$	1679m	1544s	1403sh	1588m	812w, 758sh	534m	450w
$[Mn(L)]\cdot H_2O$	1678sh	1503sh	1401sh	1587sh	815s, 757sh	526m	426w
$[FeCl(L)(H_2O)]\cdot 2H_2O$	1677sh	1503sh	1400sh	1587sh	870s, 758sh	530s	475s
$[Co(L)(H_2O)_2]\cdot 2H_2O$	1716sh	1556m	1454s	1599sh	823s, 757sh	528w	460s
$[Co(L)(H_2O)]\cdot H_2O$	1675sh	1504m	1403m	1590sh	812s, 758sh	535w	486w
$[Ni(L)]\cdot 2H_2O$	1678sh	1503sh	1405sh	1591sh	810s, 757sh	530w	464w
$[Ni(L)(H_2O)_2]\cdot H_2O$	1676sh	1503sh	1401sh	1590sh	811m, 757sh	484w	420w
$[Cu(L)]\cdot 1.5H_2O$	1675sh	1502sh	1404m	1589sh	842m, 758sh	533s	488s
$[Zn(L)]\cdot H_2O$	1679m	1508m	1401m	1595sh	812m, 758sh	530w	474s

sh = sharp, m = medium, s = small, w = weak, br = broad.

Table 3 ^{1}H NMR spectral data of H_2L and its Zn(II) complex.

Compound	δ (ppm)	Assignments
H_2L	11.641	(s, 2H, −COOH)
	8.538	(s, 2H, −CH=N)
	6.50–7.96	(m, 12H, ArH)
$[Zn(L)]\cdot H_2O$	8.477	(s, 2H, −CH=N)
	6.419–8.008	(m, 12H, ArH)
	4.15	(br, 2H, H_2O)

ing to the metal ions via the azomethine N and deprotonated carboxylate O.

3.5. ^1H NMR spectra

The chemical shifts of the different types of protons in the ^{1}H NMR spectra of the H_2L ligand and its diamagnetic Zn(II) complex are listed in Table 3. Upon comparison, the COOH signal is found at 11.641 ppm in the spectrum of H_2L ligand. This signal is completely disappeared in case of $[Zn(L)]\cdot H_2O$ complex indicating the participation of the COOH group in chelation with proton displacement. Also the signal observed at 4.15 ppm with an integration corresponding to two protons in case of Zn(II) complex, is assigned to one water molecule.

3.6. Magnetic susceptibility and electronic spectral measurements

For the hexa-coordinated Cr(III) complex, there are three spin allowed transitions i.e., ν_1: $^4A_{2g} \rightarrow {}^4T_{2g}$, ν_2: $^4A_{2g} \rightarrow {}^4T_{2g}$(F), and ν_3: $^4A_{2g} \rightarrow {}^4T_{1g}$(P) Estrela et al., 2003. The diffused reflectance spectrum of the Cr(III) chelate shows three absorption bands at 19,275 (ν_1), 26,940 (ν_2), and 28,960 cm^{-1} (ν_3). The electronic spectrum of the chelate reported here is in reasonable agreement with those in the literature (Cotton et al., 1999). The magnetic moment at room temperature is 4.05 B.M. which corresponds to the expected value for octahedral Cr(III) complexes (Cotton et al., 1999).

From the diffused reflectance spectrum it is observed that, the Fe(III) chelate exhibit a band at 21,249 cm^{-1}, which may be assigned to the $^6A_{1g} \rightarrow T_{2g}$ (G) transition in octahedral geometry of the complexes (Mohamed and Sharaby, 2007; Cotton et al., 1999). The $^6A_{1g} \rightarrow {}^5T_{1g}$ transition appears to be split into two bands at 16,746 and 14,975 cm^{-1}. The observed magnetic moment of Fe(III) complex is 5.39 B.M. Thus, the complexes formed have the octahedral geometry (Mohamed and Sharaby, 2007; Cotton et al., 1999). The spectrum shows also a band at 28,431 cm^{-1} which may attribute to ligand-metal charge transfer. The diffused reflectance spectrum of the Mn(II) complex shows three bands at 16,445, 22,965 and 27,265 cm^{-1}, which are assignable to $^6A_{1g} \rightarrow {}^4T_{1g}$, $^6A_{1g} \rightarrow {}^4T_{2g}$(G) and $^6A_{1g} \rightarrow {}^4T_{2g}$(D) transitions, respectively (Cotton et al., 1999). The magnetic moment value is 4.72 B.M. which indicates the presence of Mn(II) complex in tetrahedral structure.

The electronic spectrum of the Co(II) complex; $[Co(L)(H_2O)_2]\cdot 2H_2O$, gives three bands at 15,076, 18,674 and 22,330 cm^{-1}. The bands observed are assigned to the transitions $^4T_{1g}$ (F) $\rightarrow {}^4T_{2g}$ (F) (ν_1), $^4T_{1g}$ (F) $\rightarrow {}^4A_{2g}$ (F) (ν_2) and $^4T_{1g}$ (F) $\rightarrow {}^4T_{2g}$ (P) (ν_3), respectively, suggesting that there is an octahedral geometry around Co(II) ion (Mohamed and Sharaby, 2007; Cotton et al., 1999). The magnetic susceptibility measurements lie at 5.62 B.M. (normal range for octahedral Co(II) complexes is 4.3–5.2 B.M.), is an indicative of octahedral geometry. The band at 25,390 cm^{-1} refers to the charge transfer band.

The electronic spectrum of the Co(II) complex; $[Co(L)(H_2O)]\cdot H_2O$, resembles those of other five coordinate Co(II) complexes (Mohamed, 2006; Cotton et al., 1999), where three bands are observed at 13,280, 15,589 and 18,542 cm^{-1}. The fourth band is observed at 22,632 cm^{-1} and refers to the ligand-metal charge transfer band. The low magnetic moment value of μ_{eff} = 5.26 B.M.) is similar to that observed for the five coordinate geometry (Mohamed, 2006; Cotton et al., 1999).

The Ni(II) complex reported herein ($[Ni(L)(H_2O)_2]\cdot H_2O$) has a room temperature magnetic moment value of 3.67 B.M.; which is in the normal range observed for octahedral Ni(II) complexes (μ_{eff} = 2.9–3.3 B.M.) (Mohamed and Sharaby, 2007; Cotton et al., 1999). The electronic spectrum, in addition to showing the π–π^* and n–π^* bands of free ligands, it displays three bands, in the solid reflectance spectrum at ν_1: 15,698 cm^{-1}: $^3A_{2g} \rightarrow {}^3T_{2g}$; ν_2: 17,422 cm^{-1}: $^3A_{2g} \rightarrow {}^3T_{1g}$(F) and ν_3: 20,202 cm^{-1}: $^3A_{2g} \rightarrow {}^3T_{1g}$(P). The spectrum shows also a band at 23,655 cm^{-1} which may be attributed to the ligand-metal charge transfer.

The Ni(II) complex; $[Ni(L)]\cdot 2H_2O$, has a lower magnetic susceptibility than expected for a tetrahedral complex (West et al., 1999) due to the tetradentate H_2L ligand coordinating as a planar ligand. The diffused reflectance spectrum shows two bands at 6990 and 17,730 cm^{-1} which are assigned to $^3T_1 \rightarrow {}^3A_1$ and $^3T_1 \rightarrow {}^3T_1$(p) transitions, respectively, confirming tetrahedral structure of Ni complex (West et al., 1999).

The μ_{eff} value of the Cu(II) complex of 1.93 B.M. indicates a square planar geometry. In confirmation of this structure only one band is seen in the spectrum around 14,250 cm^{-1} with two shoulders on either sides at 18,450 and 11,205 cm^{-1}. These are assigned to $^2B_{1g} \rightarrow {}^2A_{1g}$, $^2B_{1g} \rightarrow {}^2B_{2g}$ and $^2B_{1g} \rightarrow {}^2E_{2g}$ transitions, respectively (Shukla et al., 1983). A moderately

Table 4 ESR parameters for H_2L metal complexes.

Complex	$g_{\parallel}$	$g_{\perp}$	[a] $g_{iso/av}$	[b] G
$[Mn(L)]\cdot H_2O$	2.160	1.858	1.959	1.127
$[FeCl(L)(H_2O)]\cdot 2H_2O$	2.471	3.761	3.331	0.267
$[Cu(L)]\cdot 1.5H_2O$	2.241	2.070	2.127	3.443

[a] $3g_{iso} = (2g_{\perp} + g_{//})$.
[b] $G = (g_{//} - 2) / (g_{\perp} - 2)$.

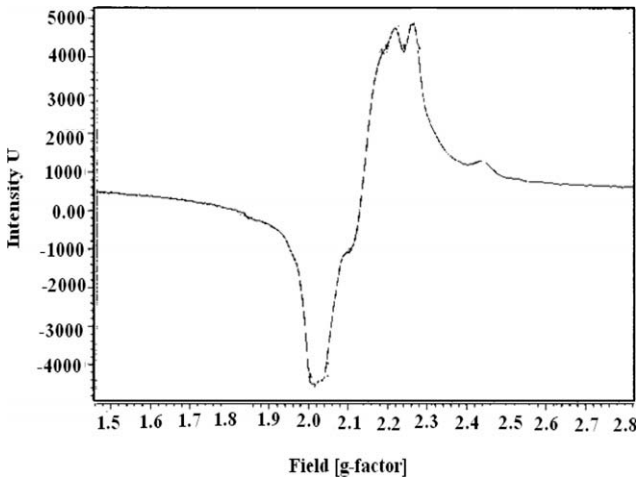

Figure 2 ESR of Cu(II)-H_2L complex.

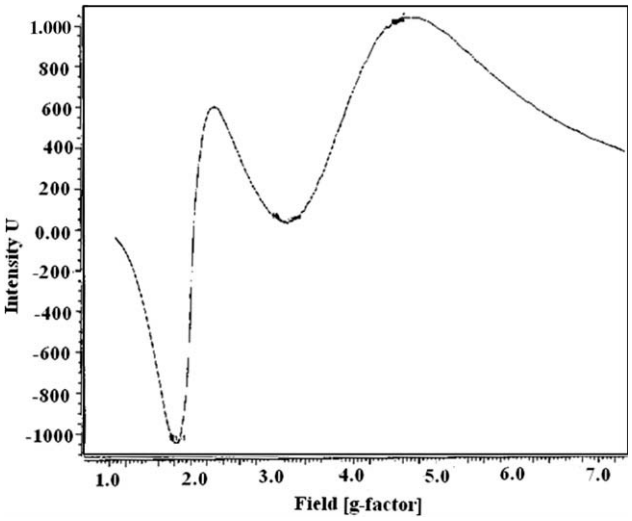

Figure 3 ESR of Mn(II)-H_2L complex.

intense peak observed at 24,364 cm^{-1} is due to ligand-metal charge transfer transition.

The Zn(II) complex is found to be accordingly diamagnetic and it is proposed to have a tetrahedral structure.

3.7. Electron spin resonance spectra

The ESR data are listed in Table 4. The ESR spectra of the Cu(II) complex at room temperature (Fig. 2) exhibits anisotropic signals with g value $g_{||} = 2.241$ and $g_{\perp} = 2.070$ (Table 4) which is characteristic for axial symmetry (Fouda and Abd-el-zaher, 2008). Since the $g_{||}$ and $g_{\perp}$ values are closer to 2 and $g_{||} > g_{\perp}$ suggesting a tetragonal distortion around the Cu(II) ion corresponding to elongation along the fourfold symmetry Z-axis (Chandra and Kuar, 2005). The trend $g_{||} > g_{\perp} > g_e$ (2.0023) shows that the unpaired electron is localized in the d_{x2-y2} orbital of the Cu(II) ion in complexes (Gudasi and Patil, 2006).

In addition, exchange coupling interaction between two Cu(II) ions is explained by Hathaway expression $G = (g_{||} - 2)/(g_{\perp} - 2)$. When the value $G < 4.0$, a considerable exchange coupling is present in solid complex ($G = 1.686$) Fouda and Abd-el-zaher, 2008. Kivelson and Neiman showed that for an ionic environment $g_{||}$ is normally 2.3 or larger, but for covalent environment $g_{||}$ are less than 2.3. The $g_{||}$ value for the Cu(II) complex is 2.241, consequently the environment is covalent (Fig. 2).

Table 5 Thermal analysis (TGA) results of H_2L and its chelates.

Complex	Temp. Range (°C)	n[#]	Mass loss % Found	Total mass loss (Calcd)	Assignment	Metallic residue
H_2L	40–1000	3.0		100.0 (100.0)	- Loss of L	———
$[CrCl(L)(H_2O)]\cdot 2H_2O$	30–120	1.0	6.82 (7.04)		- Loss of $2H_2O$.	$½Cr_2O_3$
	120–250	1.0	11.13 (10.65)		- Loss of H_2O and HCl.	
	250–1000	2.0	67.29 (67.45)	85.24 (85.14)	- Loss of L.	
$[Mn(L)]\cdot H_2O$	30–120	1.0	3.70 (4.07)		- Loss of H_2O.	
	120–900	5.0	79.16 (80.09)	82.86 (84.16)	- Loss of L.	MnO
$[FeCl(L)(H_2O)]\cdot 2H_2O$	30–110	1.0	7.19 (6.98)		- Loss of $2H_2O$.	$½Fe_2O_3$
	110–210	1.0	10.45 (10.38)		- Loss of H_2O and HCl.	
	210–1000	3.0	66.57 (67.12)	84.21 (84.48)	- Loss of L.	
$[Co(L)(H_2O)_2]\cdot 2H_2O$	40–120	1.0	7.63 (7.19)		- Loss of $2H_2O$.	CoO
	120–1000	3.0	77.01 (77.84)	84.64 (85.03)	- Loss of $2H_2O$ and L.	
$[Co(L)(H_2O)]\cdot H_2O$	30–200	1.0	8.29 (7.74)		- Loss of $2H_2O$.	CoO
	200–400	1.0	76.91 (76.13)	85.20 (83.87)	- Loss of L.	
$[Ni(L)]\cdot 2H_2O$	30–120	1.0	7.37 (7.74)		- Loss of $2H_2O$.	NiO
	120–800	3.0	75.66 (75.70)	83.03 (83.44)	- Loss of L.	
$[Ni(L)(H_2O)_2]\cdot H_2O$	30–250	1.0	11.35 (11.18)		- Loss of $3H_2O$.	NiO
	250–800	2.0	72.31 (73.29)	83.66 (84.47)	- Loss of L.	
$[Cu(L)]\cdot 1.5H_2O$	30–120	1.0	5.87 (5.86)		- Loss of $1.5H_2O$.	CuO
	120–1000	5.0	77.35 (76.87)	83.22 (82.73)	- Loss of L.	
$[Zn(L)]\cdot H_2O$	30–120	1.0	3.69 (3.97)		- Loss of H_2O.	ZnO
	120–1000	3.0	77.94 (78.15)	81.63 (82.12)	- Loss of L.	

[#] n = number of decomposition steps.

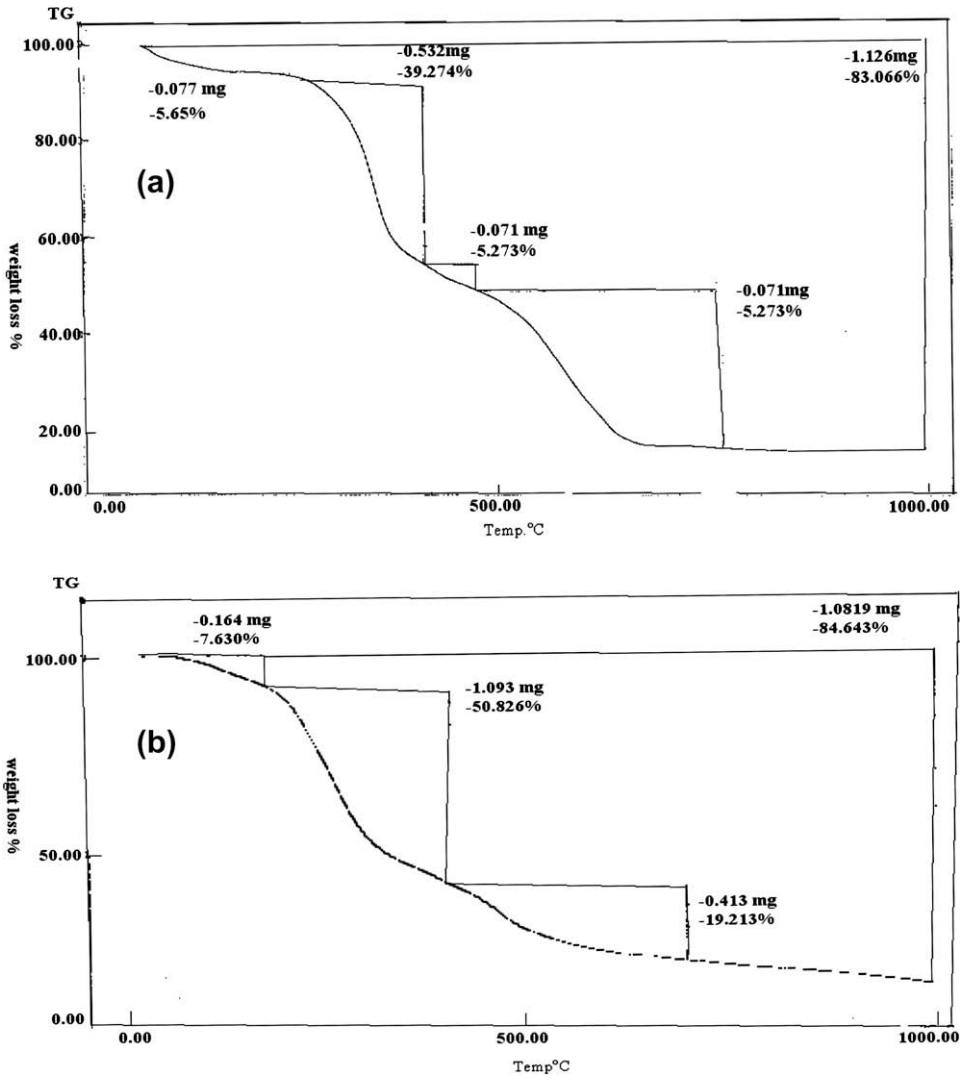

Figure 4 The TGA curves of: (a) $[Co(L)(H_2O)_2]\cdot 2H_2O$ and (b) $[Ni(L)(H_2O)_2]\cdot H_2O$.

The ESR spectra of the solid Cr(III), Co(II), Ni(II) and Zn (II) complexes at room temperature do not show ESR signal because the rapid spin lattice relaxation of the Cr(III), Co(II), and Ni(II) broadness the lines at higher temperatures (Fouda and Abd-el-zaher, 2008) and the diamagnetic nature of the Zn(II) complex. The ESR spectra show signals that may be accounted for the presence of free radicals that can resulted from the cleavage of any double bond and distribution of the charge on the two neighbor atoms. The presence of unpaired electrons from any source inside the molecule can be responsible for the appearance of these signals.

The ESR spectrum of the Mn(II) complex at room temperature (Fig. 3) gives two signals with $g_{||} = 2.160$ and $g_{\perp} = 1.858$. This finding indicates that the complex is tetrahedral which is in agreement with the data of solid reflectance and magnetic moment measurements (Fouda and Abd-el-zaher, 2008). The ESR spectrum of the [FeCl (L) $(H_2O)]\cdot 2H_2O$ complex showed two signals observed at g values 2.471 and 3.761. These values can be considered as the signal of high spin state of the Fe(III) ($S = 5/2$) (Fouda and Abd-el-zaher, 2008).

3.8. Thermal analyses (TGA and DTG)

The TGA data are listed in Table 5 and the representative TG curves are given in Fig. 4. The weight losses for each chelate were calculated within the corresponding temperature ranges. The different thermodynamic parameters are listed in Table 6.

The thermogram of H_2L ligand shows that the ligand decomposed in three successive steps within the temperature range 40–1000 °C with a total estimated mass loss 100% (calcd. mass loss = 100%). This is attributed to the loss of CO_2, $C_{17}H_{14}N_2O$, and C_4H_2 for the 1st, 2nd and 3rd steps, respectively. The thermograms of $[FeCl(L)(H_2O)]\cdot 2H_2O$ and $[CrCl(L)(H_2O)]\cdot 2H_2O$ chelates show four to five decomposition steps within the temperature range 30–1000 °C. The first two steps of decomposition within the temperature range 30–210 and 30–250 °C correspond to the loss of water molecules of hydration and coordinated and HCl gas with a mass loss of 17.64% (calcd. 17.36%) and 17.95% (calcd. 17.69%) for Fe(III) and Cr(III) complexes, respectively.

The energy values of activation are listed in Table 6. The subsequent steps (210–1000 or 250–1000 °C for Fe(III) and

Table 6 Thermodynamic data of the thermal decomposition of H_2L metal complexes.

Complex	TG range (°C)	E^* (kJ mol^{-1})	A (S^{-1})	ΔS^* (JK^{-1} mol^{-1})	ΔH^* (kJ mol^{-1})	ΔG^* (kJ mol^{-1})
$[CrCl(L)(H_2O)]\cdot 2H_2O$	30–120	35.68	4.02×10^{7}	−44.23	30.55	60.45
	120–250	60.45	6.63×10^{10}	−82.77	110.2	126.3
	250–650	92.68	6.92×10^{9}	−156.3	165.2	199.2
	650–1000	162.5	5.92×10^{11}	−184.2	179.1	220.3
$[Mn(L)]\cdot H_2O$	30–120	30.46	1.97×10^{8}	−54.29	32.38	44.56
	120–300	80.64	3.49×10^{7}	−86.96	67.96	78.96
	300–550	120.3	6.59×10^{12}	−115.1	99.72	118.5
	550–650	179.8	4.07×10^{9}	−172.2	142.5	198.8
	650–790	201.4	5.49×10^{10}	−182.6	187.2	222.7
	790–900	260.4	5.59×10^{12}	−210.6	205.1	275.2
$[FeCl(L)(H_2O)]\cdot 2H_2O$	30–110	48.65	3.88×10^{11}	−29.78	50.62	49.96
	110–210	72.25	6.55×10^{9}	−49.89	110.2	147.1
	210–350	117.7	2.87×10^{10}	−96.59	145.3	196.3
	350–580	165.1	6.69×10^{5}	−135.6	185.2	220.4
	580–800	210.0	4.99×10^{13}	−175.7	252.1	286.2
$[Co(L)(H_2O)_2]\cdot 2H_2O$	40–120	42.64	2.48×10^{7}	−56.32	56.92	43.99
	1200–400	130.9	3.19×10^{10}	−93.28	116.3	99.68
	400–690	168.3	7.06×10^{12}	−138.1	175.6	141.3
	690–900	220.4	6.48×10^{11}	−198.8	225.3	196.3
$[Co(L)(H_2O)]\cdot H_2O$	30–200	83.95	4.09×10^{12}	−63.98	42.66	66.86
	200–400	105.9	6.82×10^{9}	−109.5	137.6	141.7
$[Ni(L)]\cdot 2H_2O$	30–120	29.15	3.63×10^{7}	−33.83	37.99	55.42
	120–350	66.35	6.87×10^{9}	−79.68	76.32	40.53
	350–520	95.77	4.98×10^{12}	−122.3	105.4	100.2
	520–800	170.2	7.05×10^{10}	−155.3	176.9	182.3
$[Ni(L)(H_2O)_2]\cdot H_2O$	30–250	53.59	2.43×10^{10}	−33.66	48.66	49.56
	250–450	95.99	4.39×10^{7}	−89.77	106.2	98.86
	450–800	147.1	6.92×10^{12}	−172.4	166.7	162.9
$[Cu(L)]\cdot 1.5H_2O$	30–120	30.21	2.35×10^{9}	−40.15	40.21	47.36
	120–300	61.88	4.23×10^{11}	−87.88	75.16	91.99
	300–500	102.2	6.55×10^{7}	129.8	129.2	142.4
	500–680	152.4	7.89×10^{10}	−176.9	188.8	185.6
	680–850	199.2	6.39×10^{8}	202.9	245.1	253.4
	850–1000	234.5	4.56×10^{13}	265.3	287.3	302.1
$[Zn(L)]\cdot H_2O$	30–120	26.69	3.98×10^{5}	−52.55	35.26	40.96
	120–440	68.98	5.65×10^{8}	−97.87	59.17	91.88
	440–690	102.4	7.99×10^{10}	−146.9	119.2	142.4
	690–1000	182.6	6.86×10^{12}	−176.4	168.7	185.3

Cr(III) complexes, respectively) correspond to the removal of the ligand leaving ½Fe_2O_3 and ½Cr_2O_3 as a residue. The overall weight loss is given in Table 5.

The TGA curves of the Cu(II) and Mn(II) chelates show six stages of decomposition within the temperature range of 30–1000 and 30–900 °C, respectively. The first stage at 30–120 °C corresponds to the loss of water molecules of hydration with a mass loss of 5.87% (calcd. for $1.5H_2O$ = 5.86%) and 3.70% (calcd. for H_2O = 17.69%) for Cu(II) and Mn(II) complexes, respectively. While the successive steps (2nd to 5th) involve the loss of ligand molecule with a mass loss of 77.35% (calcd. 76.87%) and 79.16% (calcd. 80.09%) for Cu(II) and Mn(II) complexes, respectively. The overall weight loss amounts to 83.22% (calcd. 82.73%) and 82.86% (calcd. 84.16%) for Cu(II) and Mn(II) chelates, respectively.

On the other hand, $[M(L)(H_2O)_n]\cdot 2H_2O$ (M = Co(II) (n = 2) and Ni(II) (n = 0)) chelates exhibits four decomposition steps. The first step occurred within the temperature range 40–120 °C with an estimated mass loss = 7.63% (calcd. for $2H_2O$; 7.19%) and 7.37% (calcd. for $2H_2O$; 7.74%) for Co(II) and Ni(II) chelates, respectively. This may accounted for the loss of water molecules of hydration. The values of energy of activation for this step are listed in Table 6. As shown in Table 5, the mass losses of the remaining decomposition steps amount to 77.01% (calcd. 77.84%) and 75.66% (calcd. 75.70%) for Co(II) and Ni(II) chelates, respectively. They correspond to the total removal of L molecule leaving MO as a residue. The energies of activation for these steps are listed in Table 5.

$[Ni(L)(H_2O)_2]\cdot H_2O$ and $[Co(L)(H_2O)]\cdot H_2O$ complexes were thermally decomposed in three and two decomposition steps within the temperature range of 30–800 and 30–400 °C, respectively. The first decomposition step with an estimated mass loss of 11.35% (calcd. mass loss = 11.18%) and 8.29% (calcd. mass loss = 7.74%) within the temperature range 30–250 and 30–200 °C for Ni(II) and Co(II) complexes, respectively, may be attributed to the loss of hydrated and coordinated water molecules. The remaining decomposition steps are found within the temperature range 250–800 and 200–400 °C with an estimated mass loss of 72.31% (calcd. mass loss = 73.29%) and 76.91% (calcd. mass loss = 76.13%) which are reasonably accounted for the removal of L ligand molecule from the moiety of the complex.

The TGA curve of the Zn(II) chelate represents four decomposition steps as shown in Table 5. The first step of decomposition occurs within the temperature range 30–120 °C and corresponds to the loss of hydrated water molecule with a mass loss of 3.69% (calcd. for H_2O; 3.97%). The energy of activation for this dehydration step was 26.69 kJ mol^{-1}. The remaining steps of decomposition occur within the temperature range 120–1000 °C may be accounted for the removal of L ligand as gases. The overall weight losses are given in Table 5.

3.9. Kinetic data

The thermodynamic activation parameters of decomposition processes of dehydrated complexes namely activation energy (E^*), enthalpy (ΔH^*), entropy (ΔS^*) and Gibbs free energy change of the decomposition (ΔG^*) were evaluated graphically by employing the Coats–Redfern relation (Coats and Redfern, 1964). The data are summarized in Table 6. The activation energies of decomposition were found to be in the range 26.69–260.4 kJ mol^{-1}. The high values of the activation energies reflect the thermal stability of the complexes. The entropy of activation was found to have negative values in all the complexes which indicate that the decomposition reactions proceed spontaneously.

3.10. Structural interpretation

The structures of the complexes of Schiff base with Cr(III), Fe(III), Mn(II), Co(II) and Ni(II) (Cl and ClO_4), Cu(II), Zn(II) ions were confirmed by the elemental analyses, IR, molar conductance, magnetic, solid reflectance, ESR, ^1H NMR and thermal analysis data. Therefore, from the IR spectra, it is concluded that H_2L behaves as a binegatively tetradentate ligand coordinated to the metal ions via the azomethine N and deprotonated carboxylate O. From the molar conductance values, it is found that the complexes are non-electrolytes. On the basis of the above observations and from the magnetic and solid reflectance measurements, octahedral, tetrahedral, square planar and trigonal bipyramidal geometries are suggested for the investigated complexes. As a general conclusion, the investigated Schiff base behaves as a tetradentate and its metal complexes structures can be given as shown below (Fig. 5).

3.11. Biological activity

The main aim of the production and synthesis of any antimicrobial compound is to inhibit the causal microbe without any side effects on the patients. In addition, it is worthy to stress here on the basic idea of applying any chemotherapeutic agent which depends essentially on the specific control of only one biological function and not multiple ones. The chemotherapeutic agent affecting only one function has a highly sounding application in the field of treatment by anticancer, since most anticancers used in the present time affect both cancerous diseased cells and healthy ones which in turns affect the general health of the patients. Therefore, there is a real need for having a chemotherapeutic agent which control only one function.

In testing the antibacterial activity of these compounds (Table 7) we used more than one test organism to increase the chance of detecting antibiotic principles in the tested materials. The sensitivity of a microorganism to antibiotics and other antimicrobial agents was determined by the assay plates which incubated at 28 °C for 2 days for yeasts and at 37 °C for 1 day for bacteria.

All of the tested compounds showed a remarkable biological activity against different types of Gram-positive (*Staphylococcus aurous*), Gram-negative (*Escherichia coli*) bacteria and Fungi (*Candida albicans* and *Aspergillus flavus*). The data obtained are listed in Table 7. On comparing the biological activity of the Schiff base and its metal complexes with the standard tetracycline (antibacterial agent) and amphotricine B (antifungal agent), it is seen that:

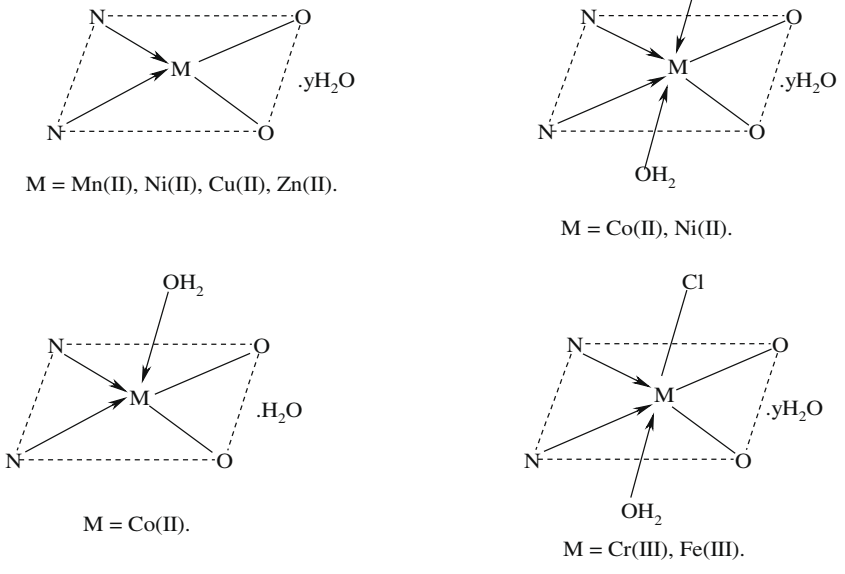

Figure 5 Structure of metal complexes.

Table 7 Biological activity of H_2L and its metal complexes.

Compound	Inhibition zone diameter (mm/mg sample)			
	Escherichia coli (G^-)	*Staphylococcus aureus* (G^+)	*Aspergillus flavus* (Fungus)	*Candida* albicans (Fungus)
H_2L	12	14	0.0	0.0
$[CrCl(L)(H_2O)]\cdot 2H_2O$	10	10	0.0	0.0
$[Mn(L)]\cdot H_2O$	11	11	0.0	0.0
$[FeCl(L)(H_2O)]\cdot 2H_2O$	10	10	0.0	0.0
$[Co(L)(H_2O)_2]\cdot 2H_2O$	17	16	0.0	14
$[Co(L)(H_2O)]\cdot H_2O$	12	12	0.0	13
$[Ni(L)]\cdot 2H_2O$	15	22	0.0	0.0
$[Ni(L)(H_2O)_2]\cdot H_2O$	11	11	0.0	0.0
$[Cu(L)]\cdot 1.5H_2O$	13	13	15	13
$[Zn(L)]\cdot H_2O$	22	21	0.0	0.0
Tetracycline (antibacterial agent)	32	34	–	–
Amphotricine B (antifungal agent)	–	–	17	21

+ diameter of inhibition zone up to 10 mm.
+ + diameter of inhibition zone 11–15 mm.
+ + + diameter of inhibition zone 16–22 mm.
+ + + + diameter of inhibition zone more than 23 mm.

(1) The biological activity of Schiff base is moderate in comparison with the standards used. It has no biological activity towards antifungal organisms.
(2) Cr(III) and Fe(III) complexes have a low activity in comparison with the Schiff base or standards. They also have no biological activity towards antifungal organisms.
(3) The remaining metal complexes have more or less biological activity that follow the order: Zn (II) > Co(II) > Ni(II) > Cu(II) > Co(II) > Schiff base > Mn(II) = Ni(II) > Fe(III) = Cr(III).
(4) It is clear also from Table 5 that Cu(II), Co(II) and Co(II) complexes have antifungal activity.

4. Conclusion

Since almost all scientists working in the field of research for new antitumours depend basically on the line of antibiotics affecting Gram-negative bacteria (Nikaido and Nakae, 1979; Brown, 1975; Hodnett et al., 1987; Hickman, 1987; El-Sharief et al., 1984), and since there are certain organisms which have proved difficult to treat and most of them are Gram-negative rods. It is therefore believed that all the complexes which are biologically active against both the Gram-negative strains may has something to do with the barrier function of the envelope of these Gram-negative strains activity, acting in a way similar to that described by Nikaido and Nakae (1979), and Brown (1975).

Therefore, it is claimed here that the synthesis of these complexes might be recommended and/or established a new line for search to new antitumour particularly when one knows that many workers studied the possible antitumour action of many synthetic and semisynthetic compounds e.g., Hodnett et al. (1987) and Hickman (1987). Such compounds may have a possible antitumour effect since Gram-negative bacteria are considered a quantitative microbiological method testing beneficial and important drugs in both clinical and experimental tumour chemotherapy (El-Sharief et al., 1984).

References

Abd El Wahed, M.G., Nour, E.M., Teleb, S., Fahim, S., 2004. J. Therm. Anal. Cal. 76, 343.
Brown, N.R.W., 1975. Resistance of Peseudomonas Aeruginosa, vol. 71, John Wiley.
Chandra, S., Kuar, U., 2005. Spectrochim. Acta 61A, 219.
Chantarasiri, N., Ruangpornvisuti, V., Muangsin, N., Detsen, H., Mananunsap, T., Batiya, C., Chaichit, N., 2004. J. Mol. Struct. 701, 93.
Coats, A.W., Redfern, J.P., 1964. Nature 20, 68.
Cotton, F.A., Wilkinson, G., Murillo, C.A., Bochmann, M., 1999. Advanced Inorganic Chemistry, sixth ed. Wiley, New York.
Elerman, Y., Kabak, M., Elmali, A., 2002. Z. Naturforsch. B 57, 651.
El-Sharief, A.M.S., Ammar, M.S., Mohammed, Y.A., 1984. Egypt J. Chem. 27 (4), 535.
Estrela dos Santos, J., Dockal, E.R., Cavalheiro, E.T.G., 2003. J. Therm. Anal. Cal. 79, 243.
Fouda, M.F.R., Abd-el-zaher, M.M., Shadofa, M.m.E., El Saied, F.A., Ayad, M.I., El Tabl, A.S., 2008. Trans. Met. Chem. 33, 219.
Grayer, R.J., Harbone, J.B., 1994. Photochemistry 73, 19.
Gudasi, K.B., Patil, S.A., Vadavi, R.S., Shenoy, R.V., 2006. Trans. Met. Chem. 31, 586.
Hickman, J.A., 1987. Biochemie 60, 997.
Hodnett, E.M., Wu, A.W., French, F.A., 1987. Eur. J. Med. Chem. Chem. Therapeut. 13, 577.
Irob, O.N., Moo-Young, M., Anderson, W.A., 1996. Int. J. Pharmacol. 34, 87.
Kaizer, J., Zsigmond, Z., Ganszky, I., Speier, G., Giorgi, M., Reglier, M., 2007. Inorg. Chem. 46, 4660.
Karabocek, S., Guner, S., Karabocek, N.J., 1997. Inorg. Biochem. 66, 57.
Kaushik, N.K., Mishra, A.K., 2003. Ind. J. Chem. 42A, 2762.
Khalil, M.M.H., Aboaly, M.M., Ramadan, R.M., 2005. Spectrochim. Acta 61A, 157.
Manav, N., Gandhi, N., Kaushik, N.K., 2000. J. Therm. Anal. Cal. 61, 127.
Mishra, A.K., Manav, N., Kaushik, N.K., 2005. Spectrochim. Acta 61A, 3097.
Mohamed, Gehad G., 2006. Spectrochim. Acta A 64, 188.
Mohamed, Gehad G., Sharaby, C.M., 2007. Spectrochim. Acta 66A, 949.

Nikaido, H., Nakae, T., 1979. Adv. Microbiol. Physiol. 20, 163.
Patel, N.H., Parekh, H.M., Patel, M.N., 2005. Trans. Met. Chem. 30, 13.
Shukla, P.R., Singh, V.K., Jaiswal, A.M., Narain, G., 1983. J. Indian Chem. Soc. LX, 321–324.
Singh, N.K., Srivastava, A., Sodhi, A., Ranjan, P., 2000. Trans. Met. Chem. 25, 133.
Sixt, T., Kaim, W., 2000. Inorg. Chim. Acta 300, 762.
Soliman, A.A., 2001. J. Therm. Anal. Cal. 63, 221.
Soliman, A.A., Mohamed, Gehad G., 2004. Thermochim. Acta 421, 151.
Sonmez, M., Levent, A., Sekerci, M., 2003. Synth. React. Inorg. Met.: Org. Chem. 33, 1747.
Tas, E., Aslanoglu, M., Ulusoy, M., Guler, M., 2004. Polish J. Chem. 78, 903.
Tian, Y.P., Duan, C.Y., Zhao, C.Y., You, X.Z., Mak, T.C.W., Zhang, Z., 1997. Inorg. Chem. 36, 1247.
Vaghasiya, Y.K., Nair, R., Soni, M., Baluja, S., Chanda, S., 2004. J. Serb. Chem. Soc. 69, 991.
West, D.X., Swearingen, J.K., Martinez, J.V., Ortega, S.H., El-Sawaf, A.K., Van Meurs, F., Castineiras, A., Garcia, I., Bermejo, E., 1999. Polyhedron 18, 2919.